Biogeosciences Discuss., https://doi.org/10.5194/bg-2018-459
Manuscript under review for journal Biogeosciences
Discussion started: 12 November 2018
© Author(s) 2018. CC BY 4.0 License.

Biogeosciences Discussions

Arctic (Svalbard Islands) Active and Exported Diatom Stocks and Cell Health Status

Susana Agustí[1,*], Jeffrey W. Krause[2,3], Israel A. Marquez[2,3], Paul Wassmann[4], Svein Kristiansen[4], and Carlos M. Duarte[1,5]

[1] King Abdullah University of Science and Technology, Thuwal, 23955-6900, Kingdom of Saudi Arabia
[2] Dauphin Island Sea Lab, Dauphin Island, 36528-4603 United States
[3] Department of Marine Sciences, University of South Alabama, Mobile, 36688-0002 United States
[4] Department of Arctic and Marine Biology, UiT The Arctic University of Norway, 9037 Tromsø, Norway
[5] Arctic Research Centre, Department of Biosscience, Aarrhus University, C.F. Mollers Alle 8, DK-8000 Arhus C, Denmark

* *Correspondence to:* Susana Agustí (sagusti@kaust.edu.sa)

Abstract. Diatoms tend to dominate the Arctic spring bloom, a key event in the ecosystem. Large sinking of diatoms is expected at the end of the bloom driven by deteriorated cell status associated to nutrients (silicon) depletion. However, there are few reports on the status of diatoms' health during Arctic blooms and its possible role on sedimentary fluxes. Here we quantify, using the Bottle-Net, Arctic diatom stocks below and above the photic layer and assess their cell health status. The communities were sampled around the Svalbard Islands and encompassed a broad diversity of conditions and bloom stages. About 1/4 (mean±SE 24.2 ± 6.7 %) of the total water column (max. 415 m) diatom stock was found below the photic layer, indicating significant sinking of diatoms in the area. The fraction of living diatom cells in the photic layer averaged 59.4 ± 6.3 % but showed the highest percentages (72.0 %) in stations supporting active blooms. In contrast, populations below the photic layer were dominated by dead cells (20.8 ± 4.9 % living cells). The percentage of diatom's stock found below the photic layer was negatively related to the percentage of living diatoms in the surface, indicating that healthy populations remained in the surface layer. An experiment on board in a tall (1.35 m) sedimentation column confirmed that dead diatom cells from the Arctic community sank faster that living ones. Also, diatoms cell mortality increased in darkness, showing an averaged half life of 1.025 ± 0.075 d^{-1}. The results conform to a conceptual model where diatoms grow during the bloom until silicic acid stocks are depleted, and support a link between diatom cell health status and sedimentation fluxes in the Arctic. Healthy arctic phytoplankton communities remained at the photic layer, whereas dying communities exported a large fraction of the biomass to the aphotic zone, fuelling carbon sequestration and benthic ecosystems.

Biogeosciences Discuss., https://doi.org/10.5194/bg-2018-459
Manuscript under review for journal Biogeosciences
Discussion started: 12 November 2018
© Author(s) 2018. CC BY 4.0 License.

1. Introduction

Diatoms can support most of the Arctic primary production during the spring phytoplankton bloom (Krause et al. 2018), the key event setting the ecosystem and driving the intense carbon uptake characteristic of the Arctic (Vaquer-Sunyer et al. 2013). However, silicic acid concentrations [$Si(OH)_4$] are characteristically low in the European Sector of the Arctic, due to the inflow of Si-depleted Atlantic water (Rey 2012). Recently, Krause et al. (2018) showed diatoms to be limited by [$Si(OH)_4$] at the spring bloom and suggested that silicon limitation could collapse a diatom bloom before nitrogen when spring conditions favor diatoms, instead of the haptophyte *Phaeocystis*.

The termination of the Arctic spring bloom is characterized by rapid sinking of diatom cells, leading to high sedimentary fluxes in the spring (Oli et al., 2002; Wassmann et al., 2006; Bauerfeind et al., 2009), precluding the production from being recycled in the upper ocean. The apparent rapid sinking of the senescent diatom bloom is, thus, responsible for the depletion of CO_2 in surface waters, with average pCO_2 values below 300 ppm and values as low as 100 ppm reported in the European sector of the Arctic (Takahashi et al., 2002; Holding et al., 2015) suggests driving strong atmospheric CO_2 uptake (Bates et al., 2009).

Current understanding of spring diatom-bloom dynamics in the Arctic suggest that rapid sinking of diatoms at the end of the Arctic spring bloom is driven by a deterioration of cell status, leading to cell mortality. However, there are few published reports on the status of diatoms' health in the arctic during Arctic blooms and the possible role deteriorated cell health status with silicon depletion may play in driving sedimentary fluxes. Alou-Font et al. (2016) found large variability in the health status of phytoplankton in the Canadian Arctic, influenced by the light and temperature conditions, but not by nitrate concentration. Because of diatoms' obligate silicon requirement, its depletion in the water column would exclusively affect their physiology, potentially their biogeochemical fate. Use of sediment traps, which are the tools used to explore diatom's sinking fluxes thus far, precludes these physiological health analyses as the time required to collect cells and trap fixatives lead to mortality of all cells. Recently, however a new instrument, the Bottle-Net, a plankton net fitted inside a Rosette sampling system that can be used to collect plankton samples at depth without a prolonged deployment, was used to assess the stock and health status of microplankton in deep waters across the subtropical and tropical ocean (Agusti et al., 2015). Here we quantified, using the Bottle-Net, Arctic diatom stocks below and above the photic layer and assess their health status in communities sampled along contrasting stages of bloom development around the Svalbard Islands. We also conducted two exploratory experiments to test the hypotheses that dead diatom cells in the field sink faster than living ones, based on previous culture experiment results (Smayda, 1971), and that diatom cells die rapidly upon falling below the photic layer.

2. Methods

2.1 Sampling and study area.

Biogeosciences Discuss., https://doi.org/10.5194/bg-2018-459
Manuscript under review for journal Biogeosciences
Discussion started: 12 November 2018
© Author(s) 2018. CC BY 4.0 License.

The study was conducted between May 17 and 29 of 2016 on board the R/V *Helmer Hanssen*. The cruise started in the southwestern fjords of Svalbard Islands transited northward toward Erik Eriksen Strait and then south towards stations near the Polar Front and the Barents Sea (Fig. 1).

Vertical profiles with a Seabird Electronics 911 plus CTD, provided with an oxygen sensor, fluorometer, turbidity meter and PAR sensor (Biospherical/LI-CORR, SN 1060) were conducted at all stations sampled. Water samples were collected using a 12 five-liter Niskin bottles installed in a rosette sampler. Water samples were taken between the surface and the bottom (max. 500 meters) for analysis of nutrients, diatom silica, productivity, and other properties (Krause et al. 2018).

At eight of the stations (Fig.1) microphytoplankton samples were collected by using two Bottle-Net devices installed in the rosette sampler. The Bottle-Net is a new oceanographic device developed for the Malaspina 2010 Circumnavigation Expedition, which consists of a 20-µm conical plankton net housed in a cylindrical PVC pipe and is designed to be mounted in the place of a Niskin bottle in the rosette sampler. The case is opened at the bottom to allow the water filtered through the internal plankton net to flow out, and a cover on the top hermetically closes or opens the bottle, remotely through the rosette mechanism, to expose the upper opening of the net (Agusti et al 2015). The Bottle-Net is lowered mounted on the rosette sampling system with the top cover closed, and this is opened at the desired bottom depth (D_b, m) of the tow, which is conducted during the ascension of the rosette, with the top cover closed again at the upper depth (D_u, m) of the water column to be sampled. This results in one integrated sample, from D_b to D_u, per deployment. Two Bottle-Nets were used mounted in the rosette sampling system, one to collect phytoplankton at the aphotic zone and the second to collect the community in the upper water column. The two layers were selected by combining the information on light penetration (PAR sensor) and chlorophyll *a* fluorescence obtained during the downward CTD cast. The upper layer included the thickness of the photic layer to the depth when chlorophyll fluorescence faded away, which typically corresponded with very low levels of PAR (below the1% of surface irradiance). The aphotic zone was selected as the layer starting ten meters below the depth of the upper layer. When the rosette reached the maximum depth at each station, one Bottle-Net was remotely opened and started filtering water until rising to the upper target depth for the aphotic zone, when it was closed. The second Bottle-Net was opened at the bottom of the photic layer and maintained open until reaching the water surface. Once on deck, the Bottle-Nets were softly rinsed with filtered seawater in order to retrieve the sample from the collector. Sampled volume was estimated as the product between the cross-sectional area of the mouth of the Bottle-Net and the vertical distance covered by the device from the start of the ascension to the closure of the top cover (D_b to D_u). The Bottle-Net presents an aspect ratio of 4, to avoid resuspension of materials filtered, displaying an efficiency of filtration of 96% for deep tows (2000-4000 m) at towing velocities around to 30 m min^{-1} (i.e. standard rosette retrieval velocities (Agusti et al., 2015).

2.2 Microplankton abundance and viability

A freshly-sampled fraction of each Bottle-Net sample was stained with the vital stain Back-light Kit (Molecular Probes ™) to identify living and dead phytoplankton cells. The Bac-light viability Kit (Molecular Probes ™ Invitrogen) is a double staining technique to test cell membrane permeability and is proven to be an effective

© Author(s) 2018. CC BY 4.0 License.

method for determining phytoplankton viability (Llabrès and Agusti 2008, Agustí et al. 2015). When excited with blue light under the epifluorescence microscope, living phytoplankton cells with intact membranes fluoresce green (Syto 9, nucleic acid stain) and dead phytoplankton cells with compromised membranes fluoresce red (Propidium Iodine, nucleic acid stain). The freshly-collected samples were filtered onto black Nucleopore of 0.8µm pore size filters, stained with the Bac-light viability Kit, placed in slides and maintained frozen at -80°C until examination under epifluorescence microscopy. The samples were examined under blue light, most on board the research vessel under a Partec CyScope® high power Blue (470 nm) and Green (528 nm) led-illuminated epifluorescence microscope, and all samples were examined at the KAUST laboratory under a Zeiss AxioObserver Z1 epifluorescence led-illuminated microscope (Colibri 7 led system). The fluorescence of the stained cells is well preserved at -80°C for several months, and samples transported to the laboratory were maintained frozen during the transport. Another fraction of the sample collected by the Bottle-Net was fixed with formalin for further examination at the laboratory. The observed diatoms were classified to genera. The percentage of living or dead cells relative to the total (i.e. dead plus living) was calculated for the total community and by genera.

2.3 Decay and sinking rates of living microphytoplankton cells

The cellular mortality rates of living phytoplankton were examined at station #3 with vertical tows from the photic layer. An aliquot of the photic-layer microphytoplankton sample was resuspended in 2 L of 0.7 µm filtered surface water and incubated in the dark at 4°C for 7 days. The community was sampled at the onset of the experiment and at increasing time intervals (i.e. 1, 3, 5, and 7 days), stained fresh with the vital stain Bac-light Kit, then prepared and examined under epifluorescence microscope as described above to quantify the living cells in the community. The half-life (i.e. the time for the number of living cells to decline to 50%) and the decay rate for each living-cell population were then calculated from the decline in living cells over time.

A experiment to test whether dead cells sink faster than living cells for any one diatom taxa was run on board using a sinking column of 30 cm diameter and 1.35 m height, representing an internal volume of 95 litres. The chamber was placed on deck, filled with 20 µm-filtered seawater, and left undisturbed for ~1 hour before starting the sinking experiment. Microplankton collected in a vertical net tow (20 µm) from the photic layer of Erik Eriksen Strait, dominated by healthy diatoms (93.3 % living cells), was resuspended in 1 liter of 0.7-µm filtered seawater and carefully added at the surface of the sinking column. A fresh subsample of the initial community, which was added to the surface of the chamber, was stained with the Bac-light Kit and the diatoms were examined under the epifluorescence microscope for the quantification of the percentage of living/dead cells and community identification, as described above. The samples at the bottom of the sinking column (sampling port located 1.35 m below the surface) were collected at intervals of time of 0 (time when the sample was added at the surface), 1, 4 and 12 hours after the initial time, and stained with the Bac-light Kit and examined under the epifluorescence microscope, as described above.

Biogeosciences Discuss., https://doi.org/10.5194/bg-2018-459
Manuscript under review for journal Biogeosciences
Discussion started: 12 November 2018
© Author(s) 2018. CC BY 4.0 License.

3. Results

The stations sampled encompassed a broad diversity of conditions, including a station where the spring bloom had not yet occurred (station 4, off the Western Svalbard shelf), as indicated by low diatom stocks and high dissolved inorganic nutrient concentrations (photic layer concentrations $Si(OH)_4$ = 4.15 ± 0.04 µmol Si L^{-1}, NO_3 = 9.43 ± 0.09 µmol N L^{-1}, Table 1). All other stations sampled were characterized by comparatively depleted nutrient concentrations (photic layer concentrations $Si(OH)_4$= 0.99± 0.30 µmol Si L^{-1}, NO_3 = 1.93 ± 0.76 µmol N L^{-1}, Table 1), thereby representing communities that were either in advanced blooming stages or were senescent after blooming. Stations 6 (SW Svalbard shelf) and 8 (E Svalbard shelf) supported actively blooming diatom populations, with the highest chlorophyll *a* concentration (10.5 µg Chl *a* L^{-1} for station 8, as described in Krause et al. 2018), and a large fraction of living diatom cells (about 70%, Table 1). In contrast, Station 9 (Polar Front) supported a senescent diatom population in post-bloom phase, as indicated by depleted nutrient pools and a low percentage of living diatom cells (46.0 %, Table 1).

Taxonomic classification under epifluorescence microscopy is not particularly accurate, but we were able to unambiguously identify different diatom genera, and some species, that dominated the microphytoplankton community. The more abundant genera found in the samples were *Thalassiosira* spp., differentiated between large (L *Thalassiosira*) and small (*Thalassiosira*) morphotypes; *Chaetoceros* spp*.,* with a large representation of *Chaetoceros socialis;* pennate diatoms including colonies of *Fragilariopsis* spp., *Navicula pelagica, Pseudo-nitzschia* sp., less abundant but identifiable cells of *Amphiprora hyperborean*, and *Coscinodiscus* sp. among others.

The living (green fluorescence) and dead (red fluorescence) cells were clearly identified under the LED-illumination of the epifluorescence microscopes used (Fig. 2). The fraction of living diatom cells in the photic layer averaged 59.4 ± 6.3 %, but ranged broadly, from 20.9 % in station 4, in pre-bloom state, to 72.0 % in station 5, which supported an active bloom. In contrast, the population sinking below the photic layer was comprised mostly of dead cells (20.8 ± 4.9 % living cells, Fig. 2). Indeed, the fraction of living diatoms was consistently greater in the photic layer than in the diatom stock sinking below the photic layer (Wilcoxon ranked sign test, P = 0.0078, Fig. 3), a pattern consistent across taxa found in at least four of the stations (large celled *Thalassiosira* sp., P = 0.02, N = 4, *Fragilariosis* sp., P = 0.005, N = 6; *Chaetoceros* sp., P = 0.0054, n = 6; Fig. 3), but the percent living cells in the photic layer and below this layer was not significantly different for the small-celled *Thalassiosira* (P = 0.09, N = 6).

The stock of diatoms that had sunk below the photic layer comprised, on average, 24.2 ± 6.7 % of the total water column stock, with this fraction ranging from 1.4 % (station 8), supporting the largest diatom bloom found, to 65.8 % of the stock at station 4, in pre-bloom status. There was a significant negative relationship between the percent of the diatom stock that had sunk below the photic layer and the percent of living cells in the photic layer (R^2 = 0.60, P = 0.02, Fig. 4), indicating that healthy, actively growing populations largely remain in the surface, whereas senescent ones sink out of the photic layer.

The suggestion that dead diatom cells sink faster than living cells was tested experimentally. Initially, only 6.7 % of the cells in the community were dead. However, all cells settling to the bottom of the sedimentation chamber within 1 h of the experiment start were dead, including large *Coscinodiscus* sp. cells (Fig. 5). The population of cells settling to the chamber bottom 4 h and 12 h following addition of the fresh, healthy community,

Biogeosciences Discuss., https://doi.org/10.5194/bg-2018-459
Manuscript under review for journal Biogeosciences
Discussion started: 12 November 2018
© Author(s) 2018. CC BY 4.0 License.

was also largely dominated by dead cells (82.2 and 71.7%, respectively, dominated by *Flagilariosis* sp. and *Thalassosira* sp. colonies), whereas the fraction of living cells retrieved in the lower sampling port after sedimentation proportionally increased with time (Fig. 5). These experimental results confirmed that dead diatom cells sink faster than living cells.

The experimental assessment of diatom survival in the dark conducted confirms that once diatom cells sink below the photic layer they die rapidly. The median (i.e. percent of living cells reduced to half) survival times in the dark were remarkably uniform across diatom taxa, ranging from 0.9 days, for *Thalassiosira* sp. to 1.2 days for *Coscinodiscus* sp., depending on species (Fig. 6). Once dead, the cells lysed; half-life periods for cell death and lysis after transfer into the dark increasing from 1.6 days, for the smaller *Flagilariosis* sp. cells, to 6.3 days for the largest *Thalasiosira* sp. cells (Fig. 6).

4. Discussion

The results presented confirm that active and healthy diatom populations, as those actively growing during the spring bloom, are associated with relatively small stocks of fast-sinking diatoms. In contrast, unhealthy diatom populations, such as those present before blooming has initiated or in the senescent phase of the bloom, characterized by a large fraction of dead cells, support comparatively larger pools of sinking diatoms.

These observations are consistent with early reports, based mostly on laboratory cultures, indicating that dead diatom cells sink faster than living ones (Smayda, 1971). The experiment conducted confirmed that dead cells sink much faster than living ones in a field assemblage with considerable diversity in species and physiological condition. Indeed, whereas the population tested was dominated by living, healthy cells, only dead cells were collected at the bottom of the sedimentation chamber over the first few hours of the experiment, and the proportion of living cells collected increased over time. Moreover, our experimental assessment of diatom survival in the dark demonstrated that once sinking below the photic layer, diatoms cells die rapidly, with half-lives in conditions in the dark of 21.8 to 30.2 hours across species. This result was consistent among the major genera and functional groups analyzed. The averaged living cells found in the photic layer were close to that described for the Canadian Arctic where the living cells in the open waters stations and ice covered stations represented the 57.3 ± 5.8% and 48.0 ± 3.9% (± SE) respectively (Alou–Font et al., 2006).

When compared across the contrasting stages of bloom development represented in the data set analyzed here, the results presented conform to a conceptual model where diatom growth during the Arctic spring bloom proceeds until silicic acid stocks are depleted (Wassmann et al., 1997; Krause et al., 2018). Silicic acid depletion leads to diatom senescent and subsequent cell death, which then results in rapid sinking of the diatom stock. For diatoms, the depletion results in two potential physiological issues: yield limitation (i.e. diatom standing stock is too high to be supported by the available silicic acid) and intense kinetic/growth limitation (i.e. depleted silicic acid silicic acid limits diatom Si uptake to such a degree that growth must slow, Krause et al., 2018). Thus, such a situation would stimulate mass sedimentation, suggested to be an evolutionary adaptation to help diatoms persist when nutrients are limiting (Raven and Waite, 2004). Diatom mortality, likely triggered by acute silicic acid limitation, is identified, therefore, as the event leading to loss of the capacity to actively regulate buoyancy that characterizes diatom cells (Smayda, 1970), and rapid sinking of the bloom.

© Author(s) 2018. CC BY 4.0 License.

Diatoms have been shown to have a remarkable metabolic capacity to regulate buoyancy (Gemmel et al., 2016), both maintaining zero (Gemmel et al., 2016) and positive buoyancy (e.g. Villareal et al., 2014) involving regulation through the production of osmolytes (Gradmann and Boyd, 2002), which plays an important role in exploiting nutrient patchiness within the photic layer (Villareal et al. 2014). Diatom sinking rates are inversely related to growth rate (Gemmel et al., 2016), so that silicon depletion is expected to result in increased sinking rates, despite field diatoms reducing their silica per cell when kinetically limited by silicic acid (McNair et al. 2018). Our results are indeed consistent with experimental demonstration that silicon depletion plays the most important role, compared to nitrogen or phosphorus, in triggering rapid sinking of diatom cells, indicating that biochemical aspects of silicon metabolism are particularly important to diatom buoyancy regulation (Bienfang et al. 1982). N:P ratios in this region do not suggest that phosphorus plays a limiting role in primary production, and when silicic acid is depleted, enough nitrate remains to fuel growth of other phytoplankton groups (e.g. *Phaeocystis*, Krause et al., 2018). Once diatoms lose their capacity to regulate buoyancy and sink below the photic layer, they die rapidly and are unable of ascending back to the photic layer, resulting in the rapid sinking fluxes that drives high sedimentation rates characteristic of the termination of the Arctic spring bloom (Oli et al., 2002; Wassmann et al., 2006, Bauerfeind et al., 2009). Rapid sinking of the Arctic spring bloom, in turn, precludes carbon recycling in the photic layer, thereby leading to undersaturated pCO_2 driving the large atmospheric CO_2 uptake characteristic of the European sector of the Arctic (Bates et al. 2009, Takahashi et al., 2002; Holding et al., 2015).

A large fraction of the total water column phytoplankton biomass was observed below the photic layer, representing on average 24% ± 6.7 (±SE) of the total diatom biomass in the study area. This considerable proportion of the phytoplankton biomass below the photic layer should be explained by a large export of diatoms sinking from the photic zone to the sea bottom. This is consistent with the high rates of biogenic silica (proxy for diatom biomass) export at stations 4, 7-8 and 10, rates were a factor of four higher than integrated diatom silica production in the upper water column and represented up to 40% of the integrated diatom silica standing stock (Krause et al., 2018). These cruise trends are in agreement with the observation of large sinking events in the Arctic as reported for ice diatoms (Boetius et al., 2014; Aumack et al., 2014) associated to ice melting in the Arctic, and that must represent a large carbon supply to benthic communities in the Arctic shelves (Moran et al., 2005; Tamelander et al., 2006). Our results show that healthy phytoplankton communities remained at the photic layer, although dying communities exported a large fraction of the biomass (up to 65%) to the aphotic zone.

In summary, the results presented here support a link between diatom cell health status and sedimentation fluxes in the Arctic. Whereas the link between diatom health status and sinking rates has long been established (Smayda, 1971), the evidence corresponded to algal cultures in the laboratory, and was lacking for natural diatom communities in this region —partially due to the logistical challenges of assessing both viability and settling in the field. Deterioration of diatom health, such as occurring when reaching acute silicon limitation (both for kinetics and yield) along the spring bloom, leads to loss of the capacity to regulate buoyancy and leads to rapid sinking, with cells exported below the photic layer dying quickly. Understanding the role of cell health status, and the role of silicic acid depletion, in the regulation of diatom sinking rates is fundamental to mechanistically understand the biological pump in the Arctic and its response to future changes.

© Author(s) 2018. CC BY 4.0 License.

Acknowledgements

This research was supported by King Abdullah University of Science and Technology through baseline funding BAS/1/1072-01-01 and BAS/1/1071-01-01 to SA and CMD, respectively; the ARCEx project funded by industry partners and the Research Council of Norway (project #228107) to PW; and funding provided by Dauphin Island Sea Lab to J. Krause. We thank the science team and crew of the R/V *Helmer Hanssen*, as well as S. Øygarden, E. Kube, A. Renner, D. Vogedes, H. Foshaug, S. Acton, D. Wiik, B. Vaaja and W. Dobbins for logistic support.

Biogeosciences Discuss., https://doi.org/10.5194/bg-2018-459
Manuscript under review for journal Biogeosciences
Discussion started: 12 November 2018
© Author(s) 2018. CC BY 4.0 License.

References

Agusti, S., González-Gordillo, J. I., Vaqué, D., Estrada, M., Cerezo, M.I., Salazar, G., Gasol, J.M. and Duarte, C. M. : Ubiquitous healthy diatoms in the deep sea confirms deep carbon injection by the biological pump, Nature Communications 6:7608. DOI: 10.1038/ncomms8608, 2015.

Alou-Font, E., Roy, S., Agustí, S. and Gosselin, M.: Cell viability, pigments and photosynthetic performance of Arctic phytoplankton in contrasting ice-covered and open-water conditions during the spring-summer transition, Marine Ecology Progress Series, 3, 543:89-106, 2016.

Aumack, C. F., A. R. Juhl, and C. Krembs. Diatom vertical migration within land-fast Arctic sea ice. Journal of Marine Systems 139 (2014): 496-504.

Bates, N. R., and Mathis, J. T. The Arctic Ocean marine carbon cycle: Evaluation of air–sea CO2 exchanges, ocean acidification impacts and potential feedbacks. Biogeosciences 6, 2433–2459, 2009.

Bauerfeind, E., Nöthig, E.-M., Beszczynska, A., Fahl, K., Kaleschke, L., Kreker, K., Klages, M., Soltwedel, T., Lorenzen, C. and Wegner, J. :Variations in vertical particle flux in the Eastern Fram Strait (79°N/4°E) during 2000-2005. Results from the Deep-Sea Long-Term observatory HAUSGARTEN, *Deep-Sea Research I* **56,** 1471-1487, 2009.

Bienfang, P. K., Harrison, P. J., and Quarmby, L. M.: Sinking rate response to depletion of nitrate, phosphate and silicate in four marine diatoms, Marine Biology, 67(3), 295-302, 1982.

Boetius, A., Albrecht, S., Bakker, K., Bienhold, C., Felden, J., Fernández-Méndez, M., ... and Nicolaus, M.: Export of algal biomass from the melting Arctic sea ice. Science, 339(6126), 1430-1432, 2013.

Gradmann D., and Boyd C.M.: Impact of osmolytes on buoyancy of marine phytoplankton, Mar Biol. ,141: 605–618, 2002.

Holding, J., Duarte, C. M., Sanz-Martín, M., Mesa, E; Arrieta, JM; Chierici, M, Hendriks, I, García-Corral, L.S., Regaudie-de-Gioux, A., Delgado, A., Reigstad, M., Wassmann, P., and Agustí, S.: Temperature dependence of CO2-enhanced primary production in the European Arctic Ocean. Nature Climate Change, 5 (12), 1079-1082, 2015.

Krause, J., Duarte, C.M., Marquez, I.A., Assmy, P., Fernandez-Mendez, M., Wiedmann, I., Wassmann, P., Kristiansen, S., and Agusti, S.: Biogenic silica production and diatom dynamics in the Svalbard region during spring. Biogeosciences Discussions, doi: 10.5194/bg-2018-226, Biogeosciences In press, 2018.

Llabrés, M., and Agustí, S.: Extending the cell digestion assay to quantify dead phytoplankton cells in cold and polar Waters, *Limnol. Oceanogr. Meth.* **6**, 659–666, 2008.

McNair, H. M., Brzezinski, M. A., Krause, J. W.:Diatom populations in an upwelling environment decrease silica content to avoid growth limitation. Environmental Microbiology, in press, 2018.

Moran, S. B., Kelly, R. P., Hagström, K., Smith, J. N., Grebmeier, J. M., Cooper, L. W., ... & Maslowski, W.: Seasonal changes in POC export flux in the Chukchi Sea and implications for water column-benthic coupling in Arctic shelves, Deep Sea Research Part II: Topical Studies in Oceanography, 52(24-26), 3427-3451, 2005.

© Author(s) 2018. CC BY 4.0 License.

Olli, K., P. Wassmann, P. Ratkova, T. Arashkevich, E. and Pasternak, A.: Seasonal variation in vertical flux of biogenic matter in the marginal ice zone and the central Barents Sea, Journal of Marine Systems, 38: 189-204, 2002.

Raven, J. A., Waite, A. M.: The evolution of silicification in diatoms: inescapable sinking and sinking as escape? New phytologist, 162(1), 45-61, 2004.

Rey, F.: Declining silicate concentrations in the Norwegian and Barents Seas, ICES Journal of Marine Science, 69, 208-212, 2012.

Smayda, T. J.: The suspension and sinking of phytoplankton in the sea, Oceanogr. Mar. Biol. 8, 353–414, 1970.

Smayda, T. J.: Normal and accelerated sinking of phytoplankton in the sea. Mar. Geol 11, 105–122 (1971).

Takahashi, T. et al.: Global sea–air CO2 flux based on climatological surface ocean pCO2 , and seasonal biological and temperature effects. Deep Sea Res. II 49, 1601–1622, 2002.

Tamelander, T., Renaud, P. E., Hop, H., Carroll, M. L., Ambrose Jr, W. G., & Hobson, K. A.: Trophic relationships and pelagic–benthic coupling during summer in the Barents Sea Marginal Ice Zone, revealed by stable carbon and nitrogen isotope measurements, Marine Ecology Progress Series, 310, 33-46, 2006.

Vaquer-Sunyer, R. et al. Seasonal patterns in Arctic planktonic metabolism (Fram Strait—Svalbard region). Biogeosciences 10, 1451–1469, 2013.

Villareal, T. A., Pilskaln, C. H., Montoya, J. P., and Dennett, M.: Upward nitrate transport by phytoplankton in oceanic waters: balancing nutrient budgets in oligotrophic seas. PeerJ, 2, e302, 2014.

Wassmann, P., Egge, J. K., Reigstad, M., and Aksnes, D. L.: Influence of dissolved silicate on vertical flux of particulate biogenic matter. Mar. Pollut. Bull. 33: 10-21,1997.

Wassmann, P., Slagstad, D., Rise CWr, and Reigstad, M.: Modelling the ecosystem dynamics of the Barents Sea including the marginal ice zone II. Carbon flux and interannual variability. Journal of Marine Systems, 59, 1-24, 2006.

© Author(s) 2018. CC BY 4.0 License.

Figure headings

Figure 1: Study area, with the insert showing the sampling locations as green dots, and labeled with the station number, around the Svalbard Islands.

Figure 2: Photographs of the natural Arctic diatoms sampled with the Bottle-Net observed under epifluorescence microscopy and stained with the Bac-light Kit. (a) Colonies of *Thalassosira* sp. showing green fluorescence corresponding to living cells. (b) Colonies of *Fragilariopsis* sp. showing dead cells (red fluorescence, vertical-left colonies) and living cells (green fluorescence, transversal-right colony). (c) Surface layer community composed by diatoms from different genera (*Chaetoceros* sp., *Fragilariopsis* sp., *Thalassiosira* sp., pennates) showing green (living cells) and red (dead cells) fluorescence. (d) Aphotic zone sample showing dead colonies (red fluorescence) of *Fragilariopsis* sp. and *Thalassiosira* sp. (two-cells colony in the bottom-right of the photo).

Figure 3: Box plots showing the distribution of the percentage of living diatoms encountered in the upper layer (blue) and aphotic zone (brown). Percentage of living cells for (a) the total diatom community and (b) for the populations of the most abundant diatom taxa observed during the cruise. The asterisks indicate significant differences between upper and aphotic layer ($p < 0.05$). Boxes encompass the central 50% of the data, the horizontal line inside the box represents the median and vertical bars encompass 90% of the data.

Figure 4: The relationship between the percentage of living diatoms cells in the photic layer and the proportion of the integrated water-column diatom stock found in the aphotic zone. The line represents the fitted linear regression ($R^2 = 0.60$, $P = 0.02$).

Figure 5: Cell viability of the diatoms quantified during the sinking experiment. The initial percentage of dead cells correspond to the fresh arctic microplankton (20 µm) sample collected at the photic layer and added to the surface of the sinking column (1.35 m height) at time 0. The percentages of dead cells at the bottom of the sinking column were collected at intervals of time of 0, 1, 4 and 12 hours after addition of the fresh population sampled.

Figure 6: Decay in the cell abundance of living (blue diamonds) and total cells (orange squares) of arctic diatoms when exposed to darkness. (a) large celled *Thalassiosira* sp. sp. (b) *Fragilariopsis* spp. (c) *Thalassiosira* sp. (d) Pennate diatom. The solid black lines and equations show the fitted linear regressions for the percent of living cells (blue box, all fitted lines significant $p < 0.05$) and total population cells (orange box, none of the fitted lines were significant $p > 0.05$).

Biogeosciences Discuss., https://doi.org/10.5194/bg-2018-459
Manuscript under review for journal Biogeosciences
Discussion started: 12 November 2018
© Author(s) 2018. CC BY 4.0 License.

Table 1. Stations number and location, averaged (±SE) photic layer temperature, salinity and nutrients, and measurements made with the Bottle-Net (BN) in the photic and aphotic zones, indicating the depth of the tows, and the abundance and percentage of living diatoms found at the two layers.

Station	Latitude °N	Longitude °E	Temperature (°C)	Salinity (psu)	$NO_3 + NO_2$ (µM)	PO_4 (µM)	$Si(OH)_4$ (µM)	BN Photic (range, m)	BN Aphotic (range, m)	Photic diatoms (cells m^{-2})	Aphotic diatoms (cells m^{-2})	Photic diatoms (% living)	Aphotic diatoms (% living)
# 3 Bellsund Hula	77 28.09	13 27.483	0.81 ± 0.33	34.4 ± 0.083	1.79 ± 1.52	0.27 ± 0.11	0.75 ± 0.45	45-0	197-55	1.30E+06	1.26E+02	63.54	21.70
# 4 Bredjupet	77 03.356	13 23.369	4.64 ± 0.025	35.0 ± 0.001	9.44 ± 0.097	0.63 ± 0.019	4.16 ± 0.046	60-0	415-100	3.04E+05	1.64E+05	20.93	9.47
# 5 Inngang Hornsund	76 58.73	15 44.113	-0.54 ± 0.035	34.2 ± 0.037	5.66 ± 0.019	0.34 ± 0.078	2.45 ± 0.40	50-0	220-80	3.20E+07	3.00E+05	72.03	0.50
# 6 Hornsund Dypet	76 51.244	15 13.143	-0.034 ± 0.1	28.9 ± 4.5	0.49 ± 0.37	0.17 ± 0.03	0.36 ± 0.118	50-0	220-60	2.01E+09	4.69E+08	70.03	8.31
# 7 Erik Eriksen Strait	79 09.986	26 02.20	-1.44 ± 0.093	34.2 ± 0.04	0.03 ± 0.026	0.16 ± 0.01	0.07 ± 0.012	50-0	260-70	1.25E+07	1.13E+06	61.12	26.99
# 8 Erik Eriksen Strait	79 10.479	26 27.518	-1.31 ± 0.088	34.2 ± 0.4	2.23 ± 1.64	0.15 ± 0.077	0.57 ± 0.40	50-0	245-70	2.47E+10	5.56E+06	69.79	31.27
# 9 Polar Front	77 15.308	29 29.243	2.04 ± 0.099	34.7 ± 0.027	0.14 ± 0.034	0.204 ± 0.022	1.29 ± 0.17	50-0	180-60	2.76E+07	2.27E+06	45.97	50.00
# 10 Barents Sea	76 13.513	29 43.710	4.06 ± 0.044	34.9 ± 0.001	3.21 ± 0.20	0.345 ± 0.03	1.48 ± 0.156	50-0	180-60	1.45E+08	2.35E+07	71.77	13.14

5

Biogeosciences Discuss., https://doi.org/10.5194/bg-2018-459
Manuscript under review for journal Biogeosciences
Discussion started: 12 November 2018
© Author(s) 2018. CC BY 4.0 License.

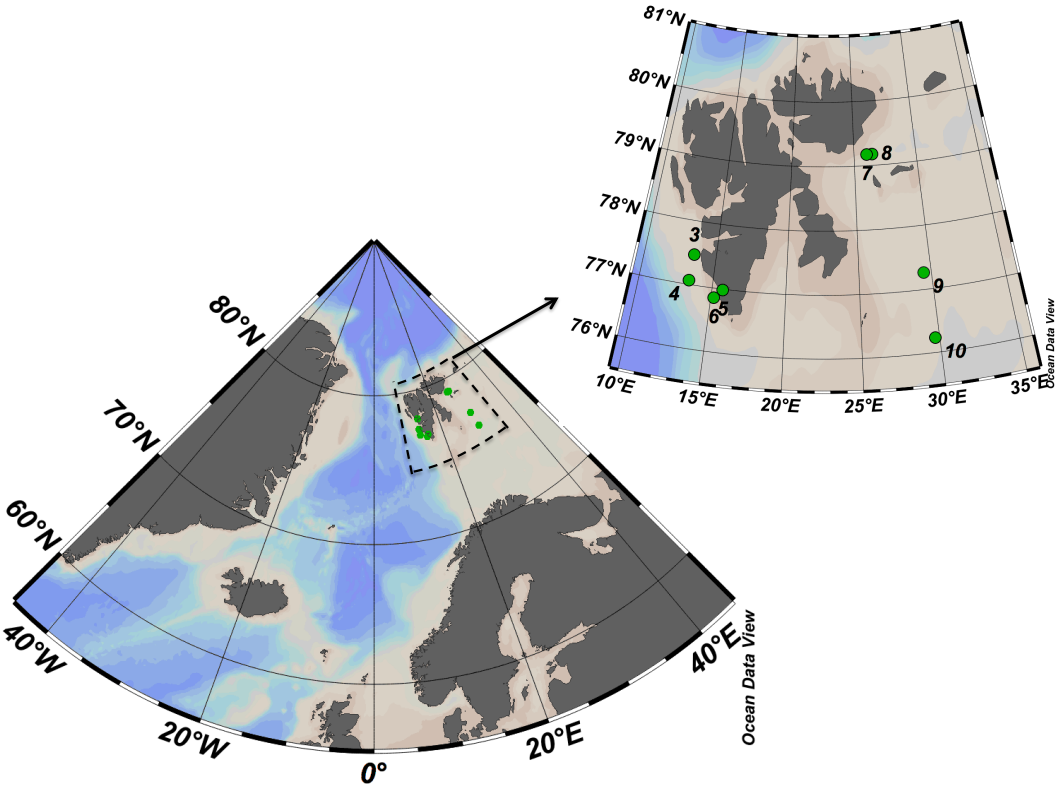

Figure 1

5

Biogeosciences Discuss., https://doi.org/10.5194/bg-2018-459
Manuscript under review for journal Biogeosciences
Discussion started: 12 November 2018
© Author(s) 2018. CC BY 4.0 License.

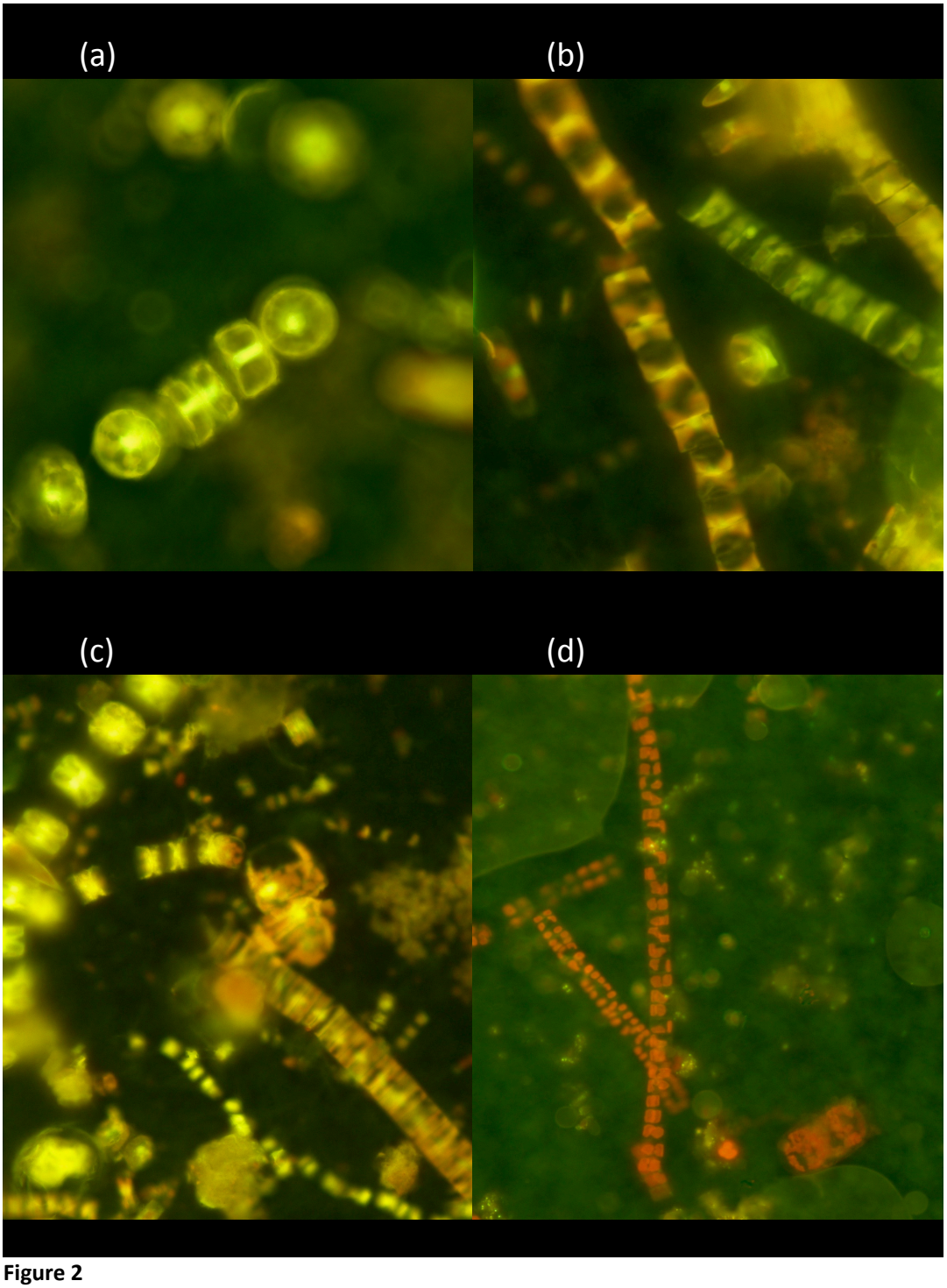

Figure 2

Biogeosciences Discuss., https://doi.org/10.5194/bg-2018-459
Manuscript under review for journal Biogeosciences
Discussion started: 12 November 2018
© Author(s) 2018. CC BY 4.0 License.

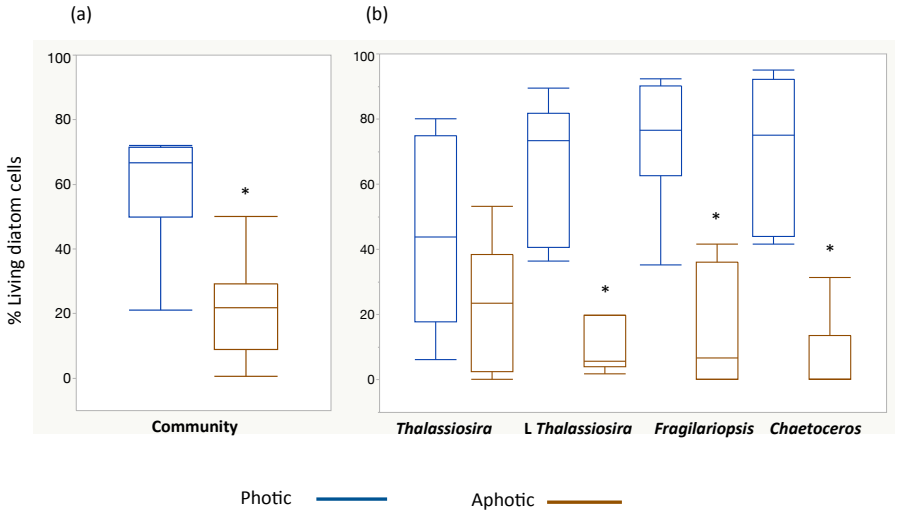

Figure 3

5

Biogeosciences Discuss., https://doi.org/10.5194/bg-2018-459
Manuscript under review for journal Biogeosciences
Discussion started: 12 November 2018
© Author(s) 2018. CC BY 4.0 License.

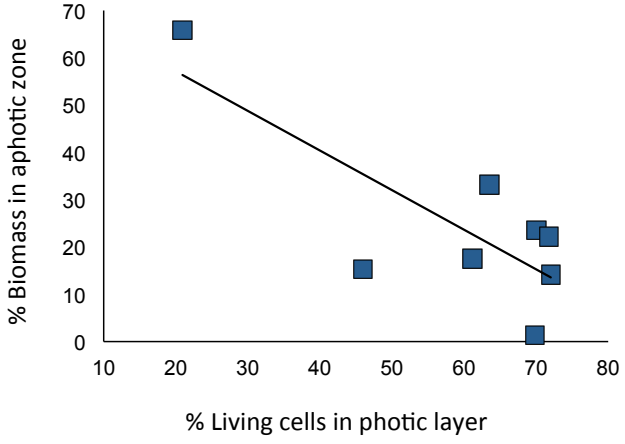

Figure 4

Biogeosciences Discuss., https://doi.org/10.5194/bg-2018-459
Manuscript under review for journal Biogeosciences
Discussion started: 12 November 2018
© Author(s) 2018. CC BY 4.0 License.

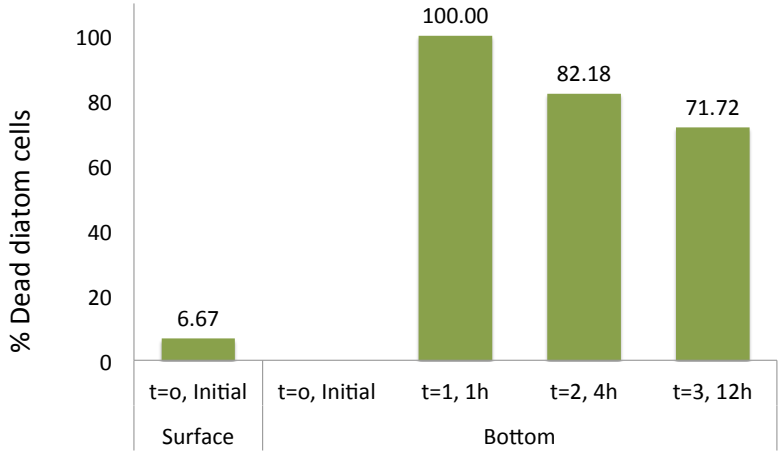

Figure 5

Biogeosciences Discuss., https://doi.org/10.5194/bg-2018-459
Manuscript under review for journal Biogeosciences
Discussion started: 12 November 2018
© Author(s) 2018. CC BY 4.0 License.

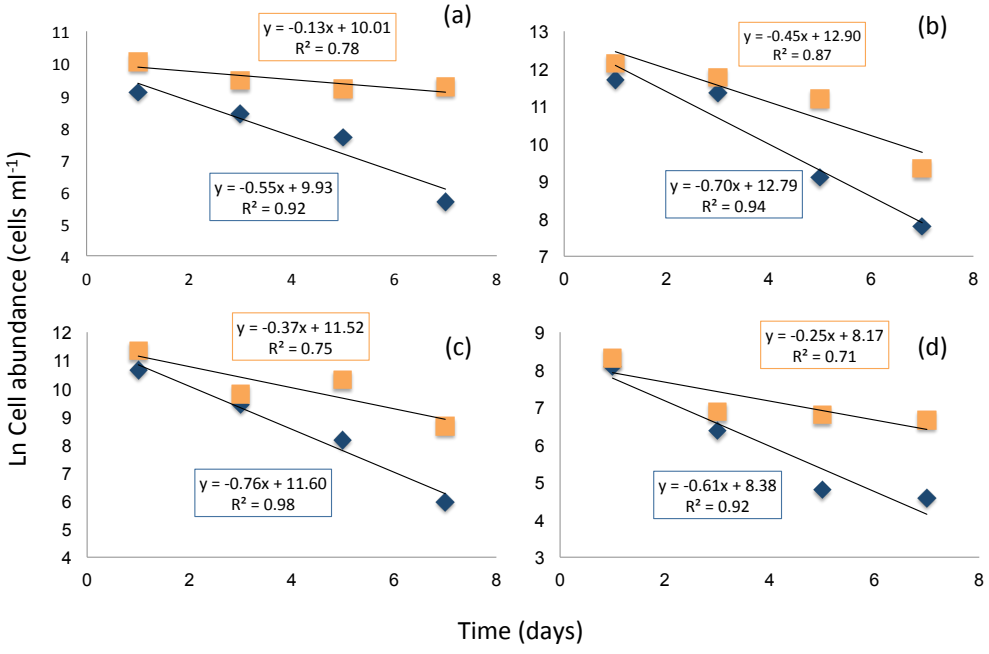

Figure 6